

Material Parameter and Effect of Thermal Load on Functionally Graded Cylinders

Sehbaz Singh¹, Dr. Sanjeev Saini²

¹Department of Mechanical Engineering, M-Tech Scholar, DAVIET Jalandhar, India.

² Department of Mechanical Engineering, DAVIET, Jalandhar, India.

ABSTRACT: The present study investigates the creep in a thick-walled composite cylinders made up of aluminum/aluminum alloy matrix and reinforced with silicon carbide particles. The distribution of SiCp is assumed to be either uniform or decreasing linearly from the inner to the outer radius of the cylinder. The creep behavior of the cylinder has been described by threshold stress based creep law with a stress exponent of 5. The composite cylinders are subjected to internal pressure which is applied gradually and steady state condition of stress is assumed. The creep parameters required to be used in creep law, are extracted by conducting regression analysis on the available experimental results. The mathematical models have been developed to describe steady state creep in the composite cylinder by using von-Mises criterion. Regression analysis is used to obtain the creep parameters required in the study. The basic equilibrium equation of the cylinder and other constitutive equations have been solved to obtain creep stresses in the cylinder. The effect of varying particle size, particle content and temperature on the stresses in the composite cylinder has been analyzed. The study revealed that the stress distributions in the cylinder do not vary significantly for various combinations of particle size, particle content and operating temperature except for slight variation observed for varying particle content. Functionally Graded Materials (FGMs) emerged and led to the development of superior heat resistant materials.

Keywords – FGM(Functionally graded material), Creep law, Von-Mises criterion, Creep Parameters,

I. Introduction

There is a development of new class of new material known as composite material, due to improvement in performance of structural components in terms of weight reduction and high strength. Nowadays composite materials are used very widely because they have desirable properties and are suitable in different situations and served their purpose very well. They are made up of two or more constituent which are in soluble and mixed at microscopic level. These are heterogeneous materials and generally used to ingredients; a binder or matrix and reinforcement (Alman, 2001). The reinforcement is stronger and hard component where as matrix act as a binder and helps reinforcement to held in its fixed place. The matrix shields the reinforcement which may be breakable like long fibers used with plastics to make fiber glass.

The composite material has high specific modulus and specific strength than that of monolithic materials. Specific modulus is the ratio of Young's modulus to density where as specific strength is the ratio of strength to the density of material for an example, the strength of graphite-epoxy unidirectional composite material is same as that of steel but specific strength of this composite material is three time more than steel and hence reducing cost of material (Kaw, 1997).

II. Functionally Graded Materials

There development of new materials for components exposed to elevated temperature and high pressure due to advancement in technology. The conventional metals alone may not survive under high thermo-mechanical loading. Thus, a new concept of Functionally Graded Materials (FGM) evolved which led to the development of superior heat resistant materials. Such new development materials have capability to resist the extreme service conditions. Functionally graded material is a type of multiphase material in which the material properties change continuously along the position to meet the design requirements of the components. There also achieve the purpose of optimizing the structure (Gupta *et al*, 2005). Functionally graded materials are extensively used in applications such as aerospace, nuclear reactors, internal combustion engines *etc.* (Noda *et al*, 1998).

The concept of FGM was first proposed by Japanese researchers in 1984-85 while they working on space plane project for advanced material in aerospace application. The body of the space craft will be undergo

a very high temperature of about 1700°C with a thermal gradient of 1000°C between inside and outside of the space craft. There was no monolithic material that can withstand such extreme temperature conditions. Therefore, the researchers proposed a concept to fabricate a material by gradually varying the material composition that led to improvement in both thermal resistance and mechanical properties.

III. Literature Review

The present study deals with creep behavior in thick-walled functionally graded cylinders exposed to operate under high service temperature and pressure. Cylinder has many industrial applications such as pressure vessels, emergency breathing cylinders, cylinders for aerospace industries, nuclear reactors and military applications, composite rotors (flywheel) *etc.* In most of these applications such as pressure vessel for storage of gases or a media transportation of high-pressurized fluids and composite rotors, the cylinder has to operate under severe mechanical and thermal loads that causes creep, and reduced service life. The high creep strength along with high specific strength offered by aluminum based metal matrix composites make them a suitable choice for these applications.

3.1 Yield Criteria

Design of any successful structural components depends upon efficient and safe use of materials. Therefore, the ability to predict the yield strength of a material *i.e.* the onset of plastic yielding, is of great practical importance for design purposes. In the field of plasticity, it is important to establish mathematical equations for determining the conditions at which yielding starts when a material is under any possible combination of loads. Further, in uniaxial loading the plastic flow begins at yield stress as in the case of tensile test. The yielding under a combined state of stress can be related to some combination of principal stresses.

The yield criteria may be expressed in terms of specific quantities, such as the stress state, the strain state, strain energy, or others. A yield criterion is usually expressed in mathematical form by means of a yield function $f(\sigma_{ij}, Y)$, where σ_{ij} is the state of stress and Y is the yield strength in uniaxial tension (or compression). The yield function is defined such that the yield criterion is satisfied when $f(\sigma_{ij}, Y) = 0$. When $f(\sigma_{ij}, Y) < 0$, the stress state is elastic. The condition $f(\sigma_{ij}, Y) > 0$ is undefined. To develop a yield function, the components of the multi-axial stress are combined into a single quantity known as the effective stress (σ_e). The effective stress is then compared with the yield stress Y , in some appropriate form, to determine if yield has occurred.

For isotropic materials, the yielding would depend on the principal stresses σ_1, σ_2 and σ_3 . For designing these materials the well-known Von-Mises (1913) yield criterion, also known as distortion-energy criterion, is used and is might be expressed as below,

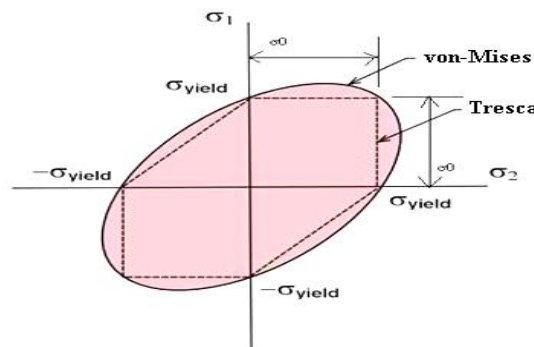
$$\sigma_e = \frac{1}{\sqrt{2}} \left[(\sigma_1 - \sigma_2)^2 + (\sigma_2 - \sigma_3)^2 + (\sigma_3 - \sigma_1)^2 \right]^{1/2}$$

Where, σ_e is equivalent stress.

For ductile materials the shear stress criterion also known as Tresca criterion, may also be used as this involved less mathematical complexity. The governing equation of shear stress criterion is given below,

$$\sigma_1 - \sigma_3 = \sigma_{yp}$$

The graphical comparison of von-Mises criterion and Tresca criterion is given below in Fig.



3.2 Variation In Distribution Of Partile Content

The silicon-carbide particles are assumed to vary linearly from the inner radius a and outer radius b , in the thick-walled functionally graded cylinder. As a result, the density of material, conductivity and creep parameters will also vary with the radius. The particle content (*vol %*) of silicon carbide $V(r)$ at any radius r is assumed to vary according to the following linear equation,

$$V(r) = V_{\max} - \frac{r-a}{b-a} [V_{\max} - V_{\min}] \quad (3.1)$$

Where, V_{\max} and V_{\min} are the maximum and minimum particle content respectively at the inner and the outer radius. In order to keep average particle content (V_{avg}) in the cylinder to be constant. One has to select either V_{\max} or V_{\min} .

Using the law of mixture, the density of FG cylinder is obtained as,

$$\rho(r) = \frac{[100-V(r)]\rho_m + V(r)\rho_d}{100} = \rho_m + \frac{(\rho_d - \rho_m)V(r)}{100} \quad (3.2)$$

here, $\rho_m = 2698.9 \text{ km/m}^3$ and $\rho_d = 3210 \text{ kg/m}^3$ are respectively the densities of pure aluminum matrix and SiCp (Metals Handbook, 1978; Clyne and Withers, 1993).

Using the value of $V(r)$ from Eqn. (4.1) into Eqn. (4.2), we obtain

$$\rho(r) = \rho_m + \frac{(\rho_d - \rho_m)(\gamma_1 - \gamma_2 r)}{100} = X - Y.r \quad (3.3)$$

)
Where,

$$X = \rho_m + (\rho_d - \rho_m) \frac{\gamma_1}{100} \quad \text{and} \quad Y = \frac{\gamma_2(\rho_d - \rho_m)}{100}$$

The average particle content (V_{avg}) in the cylinder can be expressed as,

$$V_{avg} = \frac{\int_a^b 2\pi r l V(r) dr}{\pi(b-a)l} \quad (3.4)$$

)
Where l , denotes the axial length of the composite cylinder.

Substituting the value of $V(r)$ from Eqn. (4.4) and integrating, we obtain,

$$V_{\min} = \frac{3V_{avg}(1-\psi^2)(1-\psi) - V_{\max}(1-3\psi^2 + 2\psi^3)}{(2-3\psi + \psi^3)} \quad (3.5)$$

)
Where $\psi = a/b$

3.3 CREEP LAW

In aluminum based composites, undergoing steady state creep, the effective creep rate ($\dot{\epsilon}_e$) is related to the effective stress (σ_e) through the well documented threshold stress (σ_0) based creep law given by (Mishra and Pandey, 1990; Park *et al*, 1990; Mohamed *et al*, 1992; Pandey and Mishra, 1992; Pandey *et al*, 1994.

$$\dot{\epsilon}_e = A \left(\frac{\sigma_e - \sigma_0}{E} \right)^n \exp\left(\frac{-Q}{RT} \right) \quad (3.6)$$

)
Where A , n , Q , E , R and T denotes respectively the structure dependent parameter, true stress exponent, true activation energy, temperature-dependent Young modules, gas constant and operating temperature.

The creep law given by Eqn. (3.6) may alternatively be expressed as,

$$\dot{\epsilon}_e = [M(r)(\sigma_e - \sigma_o(r))^n] \tag{3.7}$$

Where $M = \frac{1}{E} \left(A \exp \frac{-Q}{RT} \right)^{1/n}$ and the values of stress exponent n is taken as 5.

The symbols $M(r)$ and $\sigma_o(r)$ are known as creep parameters.

The creep parameters $M(r)$ and $\sigma_o(r)$ given in Eqn. (3.7) are dependent on the type of material and are also affected by temperature (T) of application. In a composite, the reinforcement size (P) and the content of reinforcement (V) are the primary material variables affecting their creep parameters. In the present study, the values of $M(r)$ and $\sigma_o(r)$ have been extracted from the uniaxial creep results reported for Al-SiCp by Pandey *et al* (1992). Though, Pandey *et al* (1992) used a true stress exponent of 8 to describe steady state creep in these composites

In order to extract the values of creep parameters for Al-SiCp, the individual set of creep data reported by Pandey *et al* (1992) have been plotted as $\dot{\epsilon}^{1/5}$ versus σ on linear scales, Figs. 4.1- 4.3. The values of creep parameters M and σ_0 have been obtained from the slope and intercept of these graphs and are reported in Table 3.1. The $\dot{\epsilon}^{1/5}$ versus σ plots corresponding to the observed experimental data points of Al-SiCp composites (Pandey *et al*, 1992) for various combinations of particle size, particle content and temperature, show an excellent linearity as evident from Figs. 4.1-4.3.

The coefficient of correlation for these plots has been reported as to 0.91 to 0.99 as given in Table 3.1.

Table 3.1: Creep parameters for Al-SiCp composites (Pandey et al, 1992)

P (μm)	T (K)	v (vol \%)	M ($s^{-1/5}/\text{MPa}$)	σ_o (MPa)	Coeff. Of correlation
1.7	623	10	0.00435	19.83	0.94
14.5	623	10	0.00872	16.50	0.99
45.9	623	10	0.00939	16.29	0.99
1.7	623	10	0.00435	19.83	0.94
1.7	623	20	0.00263	33.02	0.99
1.7	623	30	0.00227	42.56	0.94
1.7	623	20	0.00263	33.02	0.99
1.7	623	20	0.00414	29.79	0.97
1.7	723	20	0.00592	29.18	0.91

In order to determine the values of creep parameters M and σ_o for various combinations of P , V and T , reported in Table 3.1, the regression analysis has been performed by using Data-fit software. During the regression analysis, P , V and T are taken as independent variables and M and σ_o are selected as dependent variables. To accomplish the task, the creep parameters given in table have been substituted in the constitutive creep model, (4.7) to estimate the strain rates corresponding to the experimental stress values reported by Pandey *et al* (1992) for Al-SiCp composite corresponding to various combinations of material parameters and temperature as given in Table 4.1. The developed regression equations are given below,

$$M(r) = 0.02876 - \frac{0.00879}{P} - \frac{14.02666}{T(r)} + \frac{0.032236}{V(r)} \tag{3.8}$$

$$\sigma_o(r) = -0.084P - 0.0232T(r) + 1.1853V(r) + 22.2 \tag{3.9}$$

Where, P , $V(r)$, $T(r)$, $M(r)$ and σ_o respectively the particle size, particle content, temperature, creep parameter and threshold stress at any radius (r) of the FG cylinder.

In a FG cylinder, with particle content and temperature are varying along with radius. Therefore, both the creep parameters $M(r)$ and $\sigma_o(r)$ will also vary along the radius of the composite cylinder. In the present study, the particle size (P) is assumed as 1.7 μm while the temperature is assumed to vary along the radius with maximum temperature, 450 °C at internal surface and minimum temperature, 350 °C at external surface of FG cylinder. Therefore, for a given FG cylinder with known particle and thermal gradients both the creep

parameters will be functions of radius. The values of $M(r)$ and $\sigma_o(r)$ at any radius (r) could be estimated respectively from Eqs. (3.8) and (3.9) by substituting the values of particle size P , particle content $V(r)$ and operation temperature, $T(r)$ at the corresponding locations.

3.4 Temperature Gradient In The Composite Cylinder

In order to determine the temperature gradient in the composite cylinder, it is assumed that the internal and external surfaces of the cylinder are exposed to a temperature of 450°C and 350 °C respectively. To obtain the temperature of any radial distance, $T(r)$, the cylinder is divided into ten elementary cylindrical shells of equal thickness, which are, joined together and have varying thermal conductivity. For each cylindrical shell, the conductivity is assumed to be constant and determined by law of mixture as given below,

$$K(r) = \frac{[100 - V(r)]K_m + V(r)K_d}{100} \tag{3.10}$$

Where K_m (= 247 W/mK) is the matrix conductivity (Taya and Arsenault, 1989) and K_d (= 100 W/mK) is the conductivity of SiCp (Clyne and Withers, 1993).

Due to the temperature difference between the inner and outer surface of the composite cylinder the heat flux per unit length (H/l), originated, is given by (Holman, 1992),

$$\frac{H}{l} = \frac{2\pi(T_i - T_o)}{\ln(r_2/r_1)/K_1 + \ln(r_3/r_2)/K_2 + \dots + \ln(r_n/r_{n-1})/K_n} \tag{3.11}$$

Where T_i (= 450°C) is the temperature at the inner radius, and T_o (= 350°C) is the temperature at the outer radius, and K_1, K_2, \dots, K_n are thermal conductivities of different elementary cylindrical shells.

Knowing T_i and T_o , the heat flux may be estimated and afterwards the temperature of individual cylindrical shells may be estimated from the following equation,

$$T_{n+1} = T_n - \frac{H}{2\pi K_n l} \ln(r_{n+1}/r_n) \tag{3.12}$$

In the present work four different types of cylinders are assumed, as mentioned below in Table 3.2. The conductivity of these cylinders at different radius is estimated from Eqn. (3.10), and is also plotted in Fig. 4.4.

Table 3.2: Description of cylinders taken in present study

Cylinder	Particle Content and other Operating Conditions
Uniform / Non- FGM(C1)	Without particle and thermal gradients [$V_{max}= V_{min}=V_{avg} = 20 \text{ vol\%}$; $T = T_{avg}=400 \text{ }^\circ\text{C}$]. T_{avg} is the average of T_i and T_o .
Uniform / Non- FGM (C2)	With thermal gradient (TG) but without particle gradient (PG) [$V_{max}= V_{min}= V_{avg} = 20 \text{ vol\%}$].
FGM (C3)	With particle gradient (PG) but without thermal gradient (TG) [$V_{max}=25 \text{ vol\%}$; $V_{min}=16 \text{ vol\%}$; $V_{avg} = 20 \text{ vol\%}$; $T = T_{avg}=400 \text{ }^\circ\text{C}$].
FGM (C4)	With particle and thermal gradients [$V_{max}=25 \text{ vol\%}$; $V_{min}=16 \text{ vol\%}$; $V_{avg} = 20 \text{ vol\%}$].

IV. Mathematical Solution

Let us consider a thick-walled, circular cylinder made of functionally graded Al-SiCp composite. The cylinder is assumed to have inner and outer radii a and b respectively and is subjected to internal pressure p only.

The basic strain rate equations are,

$$\dot{\epsilon}_r = \frac{d\dot{\mu}}{dr} \tag{4.1}$$

$$\dot{\epsilon}_\theta = \frac{\dot{\mu}}{r} \tag{4.2}$$

Where $\dot{\mu} = \frac{d\mu}{dt}$ is the radial displacement rate and u is the radial displacement.

Where $\dot{\epsilon}_r$ and $\dot{\epsilon}_\theta$ are radial and tangential strain rates.

Eliminating, μ from Eqs. (4.13) and (4.14), the basic compatibility equation is obtained as,

$$\frac{rd\dot{\epsilon}_\theta}{dr} = \dot{\epsilon}_r - \dot{\epsilon}_\theta \quad (4.3)$$

The cylinder is subjected to following boundary conditions,

$$\text{At } r = a, \sigma_r = -p \quad (4.4)$$

$$\text{At } r = b, \sigma_r = 0 \quad (4.5)$$

Where σ_r is the radial stress.

The equilibrium equation of thick cylinder (Bhatnagar and Arya, 1969) can be written as

$$\sigma_\theta - \sigma_r = r \frac{d\sigma_r}{dr} \quad (4.6)$$

Assuming incompressibility condition (*i.e.* volume constancy condition) for creep rate, we have

$$\dot{\epsilon}_r + \dot{\epsilon}_\theta + \dot{\epsilon}_z = 0 \quad (4.7)$$

The constitutive equations of theory of creep (Bhatnagar and Arya, 1969) are given below,

$$\dot{\epsilon}_r = \frac{\dot{\epsilon}_e}{2\sigma_e} [(G + H)\sigma_r - H\sigma_\theta - G\sigma_z] \quad (4.8)$$

$$\dot{\epsilon}_\theta = \frac{\dot{\epsilon}_e}{2\sigma_e} [(F + H)\sigma_\theta - F\sigma_z - H\sigma_r] \quad (4.9)$$

$$\dot{\epsilon}_z = \frac{\dot{\epsilon}_e}{2\sigma_e} [(F + G)\sigma_z - G\sigma_r - F\sigma_\theta] \quad (4.10)$$

Where, F, G, H are anisotropic constants of the material and $\dot{\epsilon}_e$ is the effective creep rate invariant.

The von Mises (Dieter, 1998) effective stress invariant σ_e is given as below,

$$\sigma_e = \frac{1}{\sqrt{2}} [H(\sigma_\theta - \sigma_r)^2 + G(\sigma_r - \sigma_z)^2 + F(\sigma_z - \sigma_\theta)^2]^{1/2} \quad (4.11)$$

The plane strain condition is assumed *i.e.* strain rate along axial direction is zero in the present investigation,

$$\dot{\epsilon}_z = 0 \quad (4.12)$$

From Eqs. (4.13), (4.14), (4.19), displacement rate is,

$$\dot{\mu} = \frac{c}{r} \quad (4.13)$$

Where 'c' is the constant of integration.

Substituting Eqn. (4.25) in Eqn. (4.13), we get,

$$\dot{\epsilon}_r = -\frac{c}{r^2} \quad (4.14)$$

By substituting Eqn. (4.25) in Eqn. (4.14), we obtain,

$$\dot{\epsilon}_\theta = -\frac{c}{r^2} \quad (4.15)$$

Also from Eqs. (4.22) and (4.24), we have

$$\sigma_z = \frac{G\sigma_r + F\sigma_\theta}{F + G} \quad (4.16)$$

By using Eqn. (4.28) in Eqn. (4.23), the effective stress invariant (σ_e) is given by,

$$\sigma_e = \frac{1}{\sqrt{2}}(\sigma_r - \sigma_\theta) \left[\frac{FG + GH + HF}{(F + G)} \right]^{1/2} \quad (4.17)$$

Substituting the values of $(\dot{\epsilon}_r)$ and (σ_z) from Eqs. (4.26) and (4.28) in Eqn. (4.20), we obtain,

$$(\sigma_r - \sigma_\theta) = - \left[\frac{F + G}{FG + HF + GH} \right] \cdot \frac{2\sigma_e}{\dot{\epsilon}_e} \cdot \frac{c}{r^2} \quad (4.18)$$

Substituting the values of (σ_e) and $(\dot{\epsilon}_e)$ from Eqs. (4.29) and (4.7) in Eqn. (4.30), we obtain,

$$(\sigma_r - \sigma_\theta) = \frac{T}{r^{2/n}} + P \quad (4.19)$$

Where,

$$T(r) = \left[\frac{2(F + G)}{(FG + GH + HF)} \right]^{n+1} \cdot \left[\frac{-C^{1/n}}{M(r)} \right]$$

$$P(r) = \left[\frac{2(F + G)}{(FG + GH + HF)} \right]^{1/2} \cdot \sigma_0(r)$$

Solving Eqs. (4.18) and (4.31), we have,

$$-r \frac{d\sigma_r}{dr} = \frac{T(r)}{r^{2/n}} + P(r)$$

$$\frac{d\sigma_r}{dr} = - \frac{T(r)}{r^{n+2}} - \frac{P(r)}{r}$$

By integrating above expression from limit a to r , we get

$$\sigma_r = \int_a^r \frac{T(r)}{r^{n+2}} \cdot dr + \int_a^r \frac{P(r)}{r} \cdot dr + C_1 \quad (4.20)$$

Where C_1 is another constant of integration that can be evaluated by applying boundary conditions given by Eqn (4.4) in Eqn (4.20)

Therefore, Eqn (4.20) becomes,

$$\sigma_r = \int_a^r \frac{T(r)}{r^{n+2}} \cdot dr + \int_a^r \frac{P(r)}{r} \cdot dr - P \quad (4.21)$$

By applying another boundary condition given by Eqn.(4.5) in Eqn. (4.20), the constant ‘ C ’ appearing in expression of $T(r)$ can also be evaluated as below,

$$C = \frac{P - \left[\frac{2(F + G)}{(FG + GH + HF)} \right]^{1/2} \int_a^b \frac{\sigma_{(r)}}{r} \cdot dr}{\left[\frac{F + G}{(FG + GH + HF)} \right]^{n+1} \cdot \int_a^b \frac{1}{r^{n+2}} \cdot M_{(r)} \cdot dr} \quad (4.22)$$

Using, Eqs. (4.21) into Eqs. (4.19), tangential stress can be evaluated as below,

$$\sigma_\theta = \int_a^r \frac{T(r)}{r^{n+2}} \cdot dr + \int_a^r \frac{P(r)}{r} \cdot dr + \frac{T(r)}{2r^n} + P_{(r)} - P \quad (4.23)$$

Putting, Eqs. (4.23) and (4.21) in Eqs. (4.16), axial stress can be evaluated

$$\sigma_z = \int_a^r \frac{T(r)}{r^{n+2}} \cdot dr + \int_a^r \frac{P(r)}{r} \cdot dr + \frac{T(r)}{2r^n} + \frac{P(r)}{2} - P \quad (4.24)$$

4.1 Calculation Procedure

Based on analysis carried out in previous section, a mathematical model has been developed to calculate the steady state creep behavior of the rotating FGM cylinder consists of linearly decreasing SiCp particles and subjected to positive thermal gradient. For the purpose of numerical computation, the inner and outer radii of the cylinder are taken 25.4 mm and 50.8 mm respectively. The composite cylinder is subjected to internal pressure of 85.25 MPa and zero external pressures. The particle size of SiC is taken as 1.7 μm. The dimensions of cylinder selected in this study are similar to those used in earlier experimental work (Johnson *et al*, 1961) on thick-walled cylinder made of aluminum alloy. The radial, tangential and axial stresses at different radial locations of the cylinder are calculated respectively from Eqs. (4.21), (4.23) and (4.24). The creep parameters $M(r)$ and $\sigma_o(r)$ required during the computation process are estimated from Eqs. (3.8) and (3.9), for the desired combination of particle size, particle content and operating temperature. Further for isotropic cylinders, the anisotropic constants becomes equal and their value is taken as unity *i.e.* $F=G=H=1$. In order to determine the thermal gradient the temperature at inner surface is taken as 450°C and at outer surface 350°C respectively. The thermal gradient required in Eqs. (3.8) and (3.9) is estimated from Eqn. (3.12).

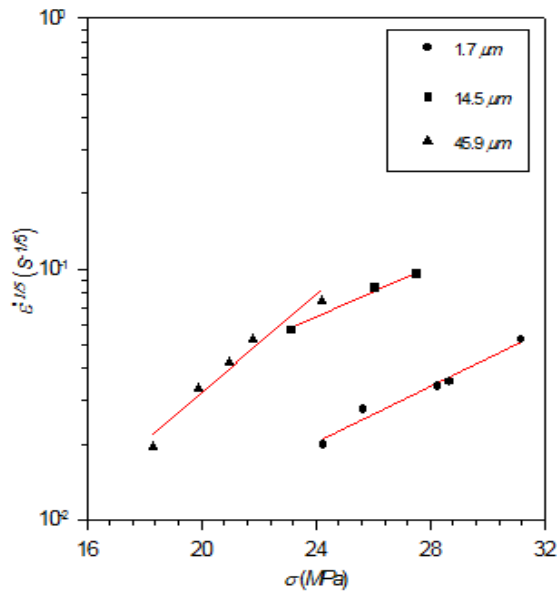


Fig. 4.1: Variation of $\dot{\epsilon}^{1/5}$ versus σ for different particle size of SiC

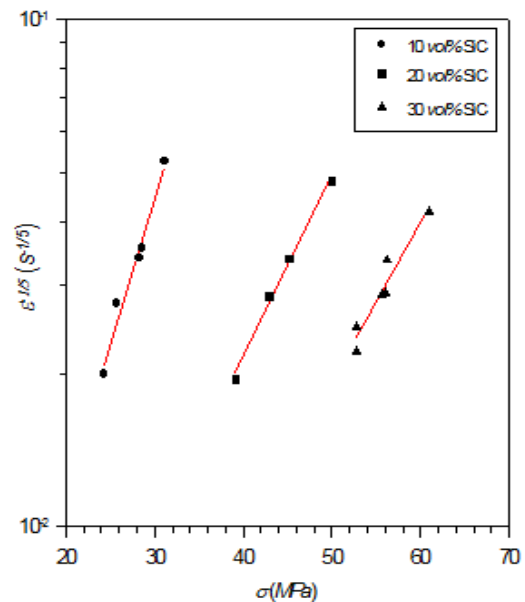


Fig. 4.2: Variation of $\dot{\epsilon}^{1/5}$ versus σ for different Volume fraction of SiC

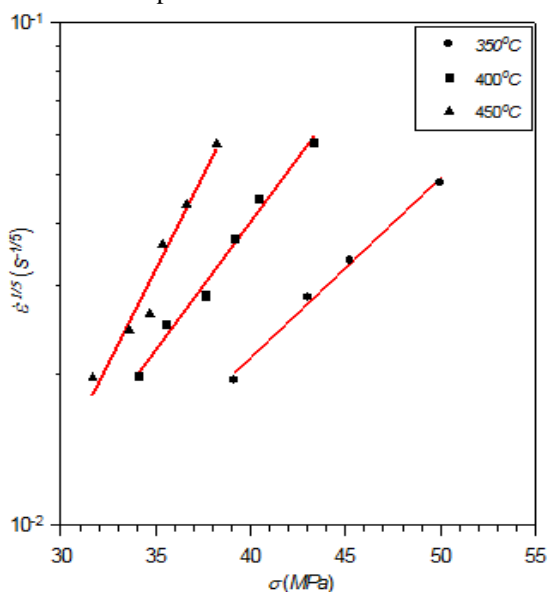


Fig. 4.3: Variation of $\dot{\epsilon}^{1/5}$ versus σ for different operating temperature.

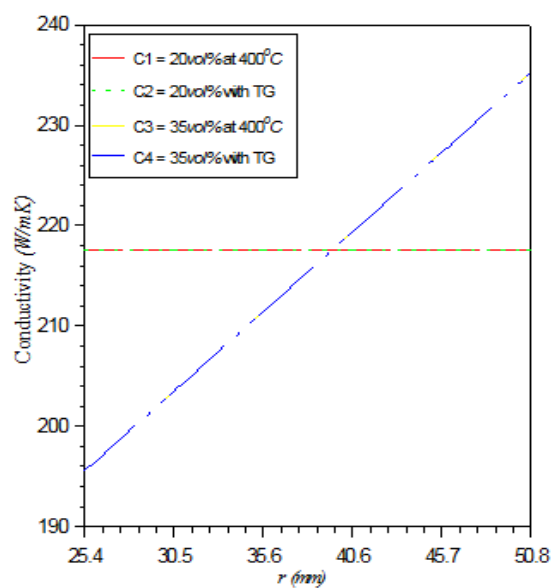


Fig. 4.4: Variation of conductivity for composite cylinders.

V. Results and Discussions

Based on the analysis, a mathematical model has been developed to obtain the stress distribution in functionally graded cylinder which has been obtained for various combinations of particle size, P , particle content, V , and temperature, T . The values of creep parameter have been taken from Table 3.1. The results have been obtained for uniform composite cylinder and functionally graded cylinders with and without thermal gradient, as mentioned in Table 3.2.

To accomplish this task, the creep rates are estimated from the present analysis for an isotropic composite cylinder made of copper for which the results are reported in the literature (Johnson *et al*, 1961). The dimensions of the cylinder, operating pressure and temperature, and the values of creep parameters used for the purpose of validation are summarized in Table 5.1.

Table 5.1: Data used for validation (Johnson *et al*, 1961)

Cylinder Material : Copper
Cylinder dimensions: $a = 25.4 \text{ mm}$, $b = 50.8 \text{ mm}$.
Internal Pressure = 23.25 MPa , External Pressure = 0
Operating Temperature = $250 \text{ }^\circ\text{C}$
Creep parameters estimated: $M = 3.271 \times 10^{-4} \text{ s}^{-1/5}/\text{MPa}$, $\sigma_0 = 11.32 \text{ MPa}$

To estimate the values of parameters M and σ_0 for copper cylinder, firstly the values of effective stress, σ_e , have been calculated at the inner and the outer radii of cylinder by substituting the values of σ_r , σ_θ and σ_z into von-Mises yield criterion given by Eqn. 4.11, as reported by Johnson *et al* (1961), at these locations. The effective stress, thus estimated at the inner radius ($\sigma_e = 189.83 \text{ MPa}$ and $\dot{\epsilon}_e = 2.168 \times 10^{-8} \text{ s}^{-1}$) and the outer ($\sigma_e = 116 \text{ MPa}$ and $\dot{\epsilon}_e = 1.128 \times 10^{-9} \text{ s}^{-1}$) of the copper cylinder are substituted in creep law, Eqn. (3.7) to obtain the creep parameters M and σ_0 for copper cylinder as given in Table 5.1. The material is isotropic, so the values of anisotropic constants, $F = G = H = 1$.

5.1 Creep Stresses and Creep Rates

To study the effect of thermal gradient and particle gradient on creep behavior of composite cylinder, the steady state stresses, have been obtained in four different composite cylinders as mentioned in Table 4.2, and are also plotted in Figs. (5.1)-(5.4). The cylinder taken for investigation in the present work (Table 5.1) is having same dimensions that of cylinder used by Johnson *et al* (1961) in their work.

The radial stress, Fig. 5.1 remains compressive (negative) throughout the cylinder, with maximum value at the inner radius (82.25 MPa) and zero at the outer radius, due to imposed boundary conditions given in Eqs. (4.4) and (4.5). The magnitude of radial stress increases throughout the cylinder when thermal gradient is imposed and due to this the variation of radial stress becomes almost linear. However, the presence of particle gradient leads to reduction in the magnitude of radial stress over the entire radial distance. The simultaneous presence of particle and thermal gradient has averaging effect on the radial stress. It can be seen from Fig. 5.1 that the maximum variation observed in the magnitude of radial stress is 5.8 MPa at a radius of 35.6 mm of composite cylinder. The tangential stress shown in Fig. 5.2 remains tensile throughout and is observed to increase linearly with increasing radial distance for uniform cylinder C1. The imposition of thermal gradient, with temperature at inner radius being higher than at the outer radius, in uniform cylinder (C2) leads to decrease in tangential stress by 29.2 MPa , near the inner radius but increase in tangential stress by 45 MPa near the outer radius as compared to those observed in cylinder C1. Further, similar to radial stress, the variation of tangential stress also becomes linear and steeper with the imposition of thermal gradient alone. By incorporating more amounts of silicon carbide particles near the inner radius, as in FG cylinder C3, the tangential stress significantly increases by 30.5 MPa near the inner radius but decreases by 47.1 MPa at the outer radius in comparison to uniform cylinder C1. Further, the tangential stress distribution becomes more uniform thereby reducing the in-homogeneity. The region having relatively more particle offers higher stress compared to the region containing lesser amount of particle. The similar observation had also been reported by Pandey *et al*, (1992) in their experimental study of Al-SiC composites. When the cylinder (C4) is subjected to particle and thermal gradients together, the tangential stress is having averaging effect and its value is in-between the values obtained for cylinder C2 and C3. The axial stress in cylinder C1 changes its nature from compressive (negative) at the inner radius and it become tensile (positive) at the outer radius as shown in Fig. 5.3. By imposing temperature gradient in uniform cylinder (*i.e.* cylinder C2), the axial stress near the inner radius becomes more compressive. Further, the tensile value of axial stress increases near the outer radius compared to that observed in uniform composite cylinder C1 at constant temperature. The imposition of particle gradient alone in uniform cylinder (*i.e.* cylinder C3) decreases the magnitude of compressive value of axial stress near the inner radius

when compared with uniform cylinder C1. The simultaneous presence of both the gradients superimposes each other to result effect similar to that observed for tangential stress in Fig. 5.2. The distribution of von-Mises effective stress is plotted in Fig. 5.4. The effect of thermal and particle gradients alone or together on variation of effective stress, Fig. 5.4, is almost opposite in nature to those observed for tangential stress in Fig. 5.2. Further, the magnitude of effective stress is also increases for the entire radial distance of the composite cylinder as compared to tangential stress values.

VI. Conclusions

- 1) The radial, tangential and axial stresses increases as we move from inner towards outer radii of cylinder, reaches maximum before decreasing near the outer radius.
- 2) The stress distribution in the cylinder does not vary significantly for various combinations of particle size and operating temperature. The increase in particle content shows sizable variation on stress distribution cylinder
- 3) The effect of imposing thermal and particle gradients, either alone or simultaneously, on the axial stress is almost similar to that observed for tangential stress in the cylinder.
- 4) The effective stress is significantly affected by incorporating particle as well as temperature gradient alone or simultaneously. The trend of variation in effective stress is opposite to that of tangential stress.

Figures:-

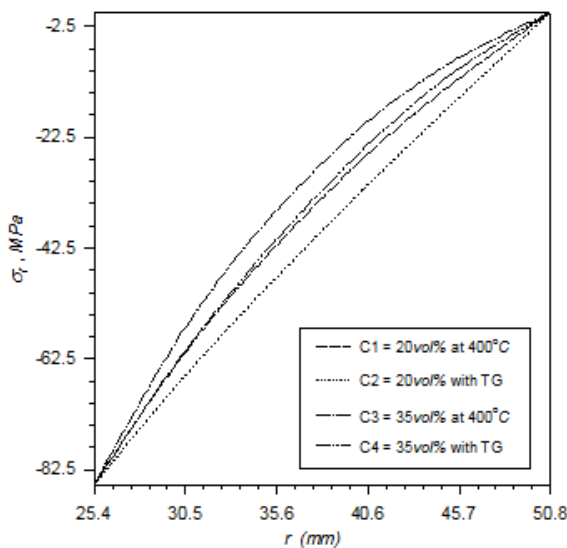


Fig 5.1: Variation of radial stress in composite cylinder.

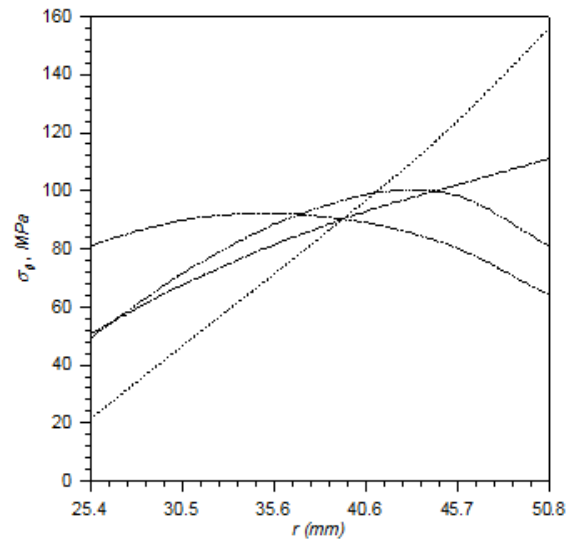


Fig 5.2: Variation of tangential stress in composite cylinder.

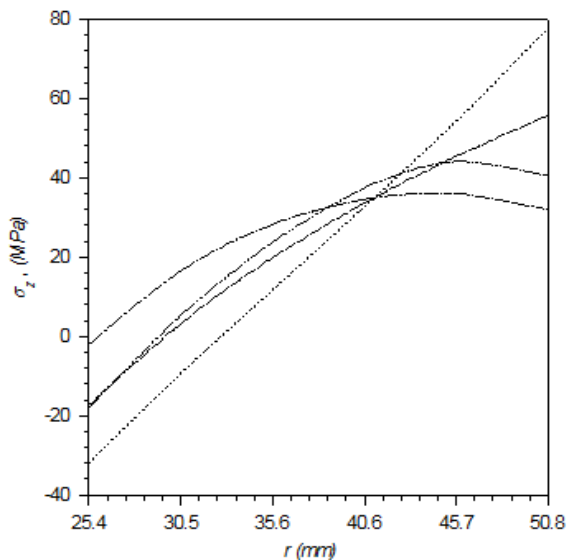


Fig 5.3: Distribution of axial stress in composite cylinder.

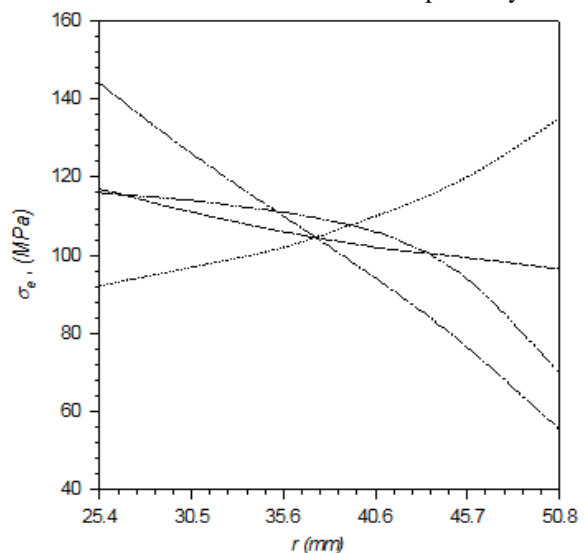


Fig 5.4: Distribution of von-Mises effective stress.

REFERENCES

- [1]. Abrinia, K., Naei, H., Sadeghi, F., and Djavanroodi, F. (2008) New analysis for the FGM thick cylinders under combined pressure and temperature loading, *American J. of Applied Sci.*, 5 (7): 852–859.
- [2]. Arya, V.K., Debonath, K.K., and Bhatnagar, N.S. (1983) Creep analysis of orthotropic cylindrical shells, *Int. J. of Pressure Vessels and Piping Technol.*, 11: 167–190.
- [3]. Bhatnagar, N.S., and Gupta, S.K. (1969) Analysis of thick-walled orthotropic cylinder in the theory of creep, *J. of Physical Soc. of Japan*, 27(6): 1655–1662.
- [4]. Bhatnagar, N.S., Arya, V.K., and Debonath, K.K. (1980) Creep analysis of orthotropic rotating cylinder, *J. of Pressure Vessel Technol.*, 102: 371–377.
- [5]. Cadek, J., Oikawa, H., and Sustek, V. (1995) Threshold creep behaviour of discontinuous aluminium and aluminium alloy matrix composites: An overview, *Mater. Sci. Engng.*, A190: 9–21.
- [6]. Cooley, W. G., and Palazotto, A. (2005) Finite element analysis of functionally graded shell panels under thermal loading, *Proceedings of the 2005 ASME International Congress and Exhibition*, Paper No. IMECE 2005–85778.
- [7]. Dieter, G.E. (1988) *Mechanical metallurgy*, London: McGraw-Hill.
- [8]. Erdogan, F., and Wu, B.H. (1993) Analysis of FGM specimens of fracture toughness testing, *Ceramic Trans.*, 34: 39–46.
- [9]. Gonzalez-Doncel, G., and Sherby, O.D. (1993) High temperature creep behaviour of metal matrix aluminium-SiC composites, *Acta Metall Mater*, 41(10): 2797–2805.
- [10]. Hagihara, S., and Miyazaki, N. (2008) Finite element analysis for creep failure of coolant pipe in light water reactor due to local heating under severe accident condition, *Nuclear Engng Design*, 238(1): 33–40.
- [11]. Hirai, T. and Chen, L. (1999) Recent and prospective development of functionally graded materials in Japan, *Mater. Sci. Forum*, 308–311: 509–514.
- [12]. Holman, J.P. (1992) *Heat transfer*, McGraw-Hill Book Company, London.
- [13]. Hulsurkar, S. (1981) Transition theory of creep of composite cylinder under uniform internal pressure, *J. of Math. and Physical Sci.*, 15(4): 377–386.
- [14]. Hyde, T.H., Yehia, K., and Sun, W. (1996) Observations on the creep of two-material structures, *The J. of Strain Analysis for Engng Design*, 31(6): 441–461.
- [15]. Ivošević, M., Knight, R., Kalidindi, S. R., Palmese, G. R., and Sutter, J. K. (2006) Solid particle erosion resistance of thermally sprayed functionally graded coatings for polymer matrix composites, *Surf. Coat. Technol.*, 200: 5145–5151.
- [16]. Jamian, Saifulnizan., Sato, Hisashia., Tsukamoto, Hideaki., and Watanabe, Yoshimi (2012) Creep analysis of functionally graded materials thick-walled cylinder, *Int. C. on Mechanical and Manufacturing Engineering*.
- [17]. Leushake, U., Krell, T., and Schulz, U. (2004) Graded thermal barrier coating systems for gas turbine applications, *Materialwiss Werkstofftech.*, 28: 391–394.
- [18]. Li, Y., and Langdon, T.G. (1999b) Fundamental aspects of creep in metal matrix composites, *Metall. Mater. Trans.*, 30A: 315–323.
- [19]. Li, Y., and Mohamed, F.A. (1997) An investigation of creep behaviour in an SiC-2124 Al composite, *Acta Mater*, 45(11): 4775–4785.
- [20]. Ma, Z.Y., and Tjong, S.C. (2001) Creep deformation characteristics of discontinuously reinforced aluminium-matrix composites, *Composites Sci Technol.*, 61(5): 771–786.
- [21]. *Metals Handbook* (1978) Vol.2, 9th Edition. American Society for Metals, Metal Park, Ohio, USA, 714.
- [22]. Mishra, J.C., and Samanta, S.C. (1981) Finite creep in thick walled cylindrical shells at elevated temperature, *Acta Mechanica*, 41: 149–155.
- [23]. Mohamed, F.A., Park, K.T., and Lavernia, E.J. (1992) Creep behaviour of discontinuous SiC–Al composites, *Mater Sci Engng.*, A150(1): 21–35.
- [24]. Noda, N., Nakai, S. and Tsuji, T. (1998) Thermal stresses in functionally graded materials of particle-reinforced composite, *JSME Int. J.* 41A (2): 178–184.
- [25]. Obata, Y., and Noda, N. (1994) Steady thermal stresses in a hollow circular cylinder and hollow sphere of a functionally graded materials, *J. Thermal Stresses*, 17: 471–487.
- [26]. Ootao, Y., and Tanigawa, Y. (2000) Three-dimensional transient piezothermoelasticity in functionally graded rectangular plate bonded to a piezoelectric plate, *Int. J. Solids Structures*, 37: 4377–4401.
- [27]. Ozturk, Ali., and Gulgec, Mufit. (2011) Elastic–plastic stress analysis in a long functionally graded solid cylinder with fixed ends subjected to uniform heat generation, *Int. J. of Engineering Science.*, 49: 1047–1061.
- [28]. Pandey, A.B., Mishra, R.S., and Mahajan, Y.R. (1992) Steady state creep behaviour of silicon carbide particulate reinforced aluminium composites, *Acta Metall Mater.*, 40(8): 2045–2052.
- [29]. Pandey, A.B., Mishra, R.S., and Mahajan, Y.R. (1994) High-temperature creep of Al-TiB₂ particulate composites, *Mater. Sci. Engng.*, A189 (1-2): 95–104.
- [30]. Perry, J., and Aboudi, J. (2003) Elasto-plastic stresses in thick walled cylinders. *ASME J. Pressure Vessel Technol.*, 125(3): 248–252.
- [31]. Rimrott, F.P.J. (1959) Creep of thick-walled tubes under internal pressure considering large strains, *J. Appl Mech.*, 26: 271–274.
- [32]. Robotnov, Y.N. (1969) *Creep problems in structural members*, Translated from Russian by Transcripta service Ltd., London, North-Holland Publishing Co. Amsterdam.
- [33]. Sherrer, R.E. (1967) Filament wound cylinders with axial- symmetric loads, *J. of Composite Mater.*, 1: 344–355.

- [34]. Spencer, A.M. (1986) Strain characterization of anisotropic material by thick ring pressure test, *Composites*, 17: 121–125.
- [35]. Tachibana, Y., Iyoku, T. (2004) Structural design of high temperature metallic components, *Nuclear Engng Design*, 233(1-3): 261–272.
- [36]. Takeuch, K., Kawazoe, M., and Kanayama, K. (2003) Design of functionally graded wood-based board for floor heating system with higher energy efficiency, *Functionally Graded Materials, Proceedings of the 7th Int. Symposium on Functionally Graded Materials (FGM2000)*, Mater. Sci. Forum, W. Pan, J. Gong, L. Zhang, and L. Chen, eds., Trans Tech Publications Ltd., Uetikon-Zuerich, Switzerland, 423–425, 819–824.
- [37]. Tauchert, T.R. (1981) Optimum design of cylindrical pressure vessel, *J. of Composite Mater.*, 15: 390–402.
- [38]. Taya, M., and Arsenault, R.J. (1989) *Metal matrix composites: Thermomechanical behaviour*, Pergamon Press, Oxford, UK, 248.
- [39]. Tjong, S.C., and Ma, Z.Y. (2000) Microstructural and mechanical characteristics of in situ metal matrix composites, *Mater Sci Engng.*, R29(3-4): 49–113.
- [40]. Tutuncu, Naki. (2006) Stresses in thick-walled FGM cylinders with exponentially-varying properties, *Engineering Structures* 29 (2007) 2032–2035.
- [41]. Tzeng, J.T. (1999) Viscoelastic response of composite overwrapped cylinders, *J. of Thermoplastic Composite Mater.*, 12(1): 55–69.
- [42]. Tzeng, J.T. (2002) Viscoelastic analysis of composite cylinders subjected to rotation, *J. of Composite Mater.*, 36(2): 229–239.
- [43]. Uemura, S. (2003) The activities of FGM on new applications, *Mater. Sci. Forum*, 423–425: 1–10.
- [44]. Von Mises, R. (1913) *Mechanics of solids in the plastically deformable state*, NASA, Technical Memorandum 88488, 1986. (Transition of Mechanik der festen koerper im plastisch-deformablem Zustand, *Nachrichten von der Koniglichen Gasellschaft der Wissenschaften*, 582–592).
- [45]. Yang, Y.Y. (1999) Stress analysis in a joint with functionally graded materials considering material creep behaviour, *Mater. Sci. Forum*, 308-311: 948–954.
- [46]. Yang, Y.Y. (2000) Time-dependent stress analysis in functionally graded materials, *Int. J. of Solids and Structures*. 37: 7593–7608.
- [47]. Yoshioka, H., Suzumura, Y., Cadec, J., Zhu, S.J., and Milicka, K. (1998) Creep behaviour of ODS aluminium reinforced by silicon carbide particulates: ODS Al–30 SiCp composite, *Mater. Sci. Engng.*, A248 (1): 65–72.
- [48]. You, L.H., Ou, H., and Zheng, Z.Y. (2007) Creep deformations and stresses in thick-walled cylindrical vessels of functionally graded materials subjected to internal pressure, *Composite Structures*, 78: 285–291.
- [49]. Zhai, P.C., Chen, G., and Zhang, Q.J. (2005) Creep property of functionally graded materials, *Functionally Graded Materials VIII (FGM2004)*, Proceedings of the Eighth International Symposium on Multifunctional and Functionally Graded Materials, Mater. Sci. Forum, O. Van der Biest, M. Gasik, and J. Vleugels, eds., Trans Tech Publications Ltd., Uetikon-Zuerich, Switzerland, 492–493: 599–604.
- [50]. Zhu, D., and Miller, R.A. (1999) Determination of creep behaviour of thermal barrier coatings under laser imposed high thermal and stress gradient conditions, *J. Mater. Res.*, Mater. Research Soc., 14(1): 146–161.